

A FAST HADRON FREEZE-OUT GENERATOR

N.S. Amelin, R. Lednicky,^y and T.A. Pocheptsov

Joint Institute for Nuclear Research,
Dubna, Moscow Region, 141980, Russia

I.P. Lokhtin, L.V. Malinina,^z and A.M. Snigirev

M.V. Lomonosov Moscow State University,
D.V. Skobeltsyn Institute of Nuclear Physics, 119992, Moscow, Russia

Iu.A. Karpenko and Yu.M. Sinyukov

Bogolyubov Institute for Theoretical Physics, Kiev, 03143, Ukraine

(Dated: February 15, 2021)

Abstract

We have developed a fast Monte Carlo procedure of hadron generation allowing one to study and analyze various observables for stable hadrons and hadron resonances produced in ultra-relativistic heavy ion collisions. Particle multiplicities are determined based on the concept of chemical freeze-out. Particles can be generated on the chemical or thermal freeze-out hypersurface represented by a parameterization or a numerical solution of relativistic hydrodynamics with given initial conditions and equation of state. Besides standard space-like sectors associated with the volume decay, the hypersurface may also include non-space-like sectors related to the emission from the surface of expanding system. For comparison with other models and experimental data we demonstrate the results based on the standard parameterizations of the hadron freeze-out hypersurface and low velocity profile under the assumption of a common chemical and thermal freeze-out. The C++ generator code is written under the ROOT framework and is available for public use at <http://uhkm.jinr.ru/>.

PACS numbers: 25.75.-q, 25.75.Gz

^A Also at S.P. Korolev, Samara State Aerospace University, Samara, 443086, Russia

^y Also at Institute of Physics ASCR, Prague, 18221, Czech Republic

^z Also at Joint Institute for Nuclear Research, Dubna, Moscow Region, 141980, Russia

I. INTRODUCTION

Ongoing and planned experimental studies of relativistic heavy ion collisions in a wide range of beam energies require a development of new event generators and improvement of the existing ones [1]. Especially for Large Hadron Collider (LHC) experiments, because of very high hadron multiplicities, one needs fairly fast Monte-Carlo (MC) generators for event simulation.

A successful but oversimplified attempt of creating a fast hadron generator motivated by hydrodynamics was done in Ref. [2, 3, 4, 5]. The present work is an extension of this approach. We formulate a fast MC procedure to generate hadron multiplicities, four-momenta and four-coordinates for any kind of freeze-out hypersurface. Decays of hadronic resonances are taken into account. We consider hadrons consisting of light u, d and s quarks only, but the extension to heavier quarks is possible. The generator code is written in the object-oriented C++ language under the ROOT framework [6].

In this article we discuss only central collisions of nuclei using the Bjorken-like and Hubble-like freeze-out parameterizations used in so-called "blast wave" [7] and "Cracow" models [8], respectively. The same parameterizations have been used in the hadron generator referred as THERMINATOR [9] that appears however less efficient than our generator (see sections II, VI).

The paper is now organized as follows. Sections II-V are devoted to the description of the physical framework of the model. In section VI, the Monte Carlo simulation procedure is formulated. The validation of this procedure is presented in section VII. In section VIII, the example calculations are compared with the Relativistic Heavy Ion Collider (RHIC) experimental data. We summarize and conclude in section IX.

II. HADRON MULTIPLICITIES

We give here the basic formulae for the calculation of particle multiplicities. We consider the hadronic matter created in heavy-ion collisions as a hydrodynamically expanding reball with the equation of state of an ideal hadron gas.

The mean number N_i of particles species i crossing the space-like freeze-out hypersurface

(x) in Minkowski space can be computed as [10]

$$N_i = \int_Z d^3(x) j_i(x) \quad (1)$$

Here the four-vector $d^3(x) = n(x) d^3(x)$ is the element of the freeze-out hypersurface directed along the hypersurface normal unit four-vector $n(x)$ with a positively defined zero component ($n^0(x) > 0$) and $d^3(x) = j^3 d^3 j^{-2}$ is the invariant measure of this element. The normal to the space-like hypersurface is time-like, i.e. $n \cdot n = 1$; generally, for hypersurfaces including non-space-like sectors, the normal can also be a space-like so then $n \cdot n = -1$. The four-vector $j_i(x)$ is the current of particle species i determined as:

$$j_i(x) = \int_Z \frac{d^3 p}{p^0} p f_i(x; p); \quad (2)$$

where $f_i(x; p)$ is the Lorentz invariant distribution function of particle freeze-out four-coordinate $x = (x^0; \mathbf{x})$ and four-momentum $p = (p^0; \mathbf{p})$. In the case of local equilibrium

$$f_i(x; p) = f_i^{\text{eq}}(p \cdot u(x); T(x); \mu_i(x)) = \frac{1}{(2\pi)^3} \frac{g_i}{\exp(p \cdot u(x) - \mu_i(x) - T(x)) \pm 1}; \quad (3)$$

where $p \cdot u = p_\mu u^\mu$, $g_i = 2J_i + 1$ is the spin degeneracy factor, $T(x)$ and $\mu_i(x)$ are the local temperature and chemical potential respectively, $u(x) = \gamma \mathbf{v}$ is the local collective four-velocity, $\gamma = (1 - v^2)^{-1/2}$, $u \cdot u = 1$. The signs \pm in the denominator account for the proper quantum statistics of a fermion or a boson, respectively.

The Lorentz scalar local particle density is defined as:

$$n_i(x) = u(x) \cdot j_i(x) = \int_Z \frac{d^3 p}{p^0} p \cdot u(x) f_i(x; p); \quad (4)$$

For a system in local thermal equilibrium, the particle density in the fluid element rest frame, where $u = (1; 0; 0; 0)$, is solely determined by the local temperature $T(x)$ and chemical potential $\mu_i(x)$ for each particle species i :

$$n_i^{\text{eq}}(T(x); \mu_i(x)) = u \cdot j_i^{\text{eq}}(x) = \int_Z \frac{d^3 p}{p^0} f_i^{\text{eq}}(p^0; T(x); \mu_i(x)); \quad (5)$$

the four-vectors in fluid element rest frames are denoted by star.

In the case of local equilibrium, the particle current is proportional to the fluid element four-velocity: $j_i^{\text{eq}}(x) = n_i^{\text{eq}}(T(x); \mu_i(x)) u(x)$. So the mean number of particles of species i is expressed directly through the equilibrated density:

$$N_i = \int_Z d^3(x) u(x) \cdot j_i^{\text{eq}}(T(x); \mu_i(x)); \quad (6)$$

In the case of constant temperature and chemical potential, $T(\mathbf{x}) = T$ and $\mu_i(\mathbf{x}) = \mu_i$, one has

$$N_i = \int_{(x)} d^3(x) u(\mathbf{x}) = \int_{(x)} d^3(x) u(\mathbf{x}; T, \mu_i) = V_e \int_{(x)} d^3(x) u(\mathbf{x}; T, \mu_i) \quad (7)$$

ie. the total yield of particle species i is determined by the freeze-out temperature T , chemical potential μ_i and by the total comoving volume V_e , so called effective volume of particle production which is a functional of the field of collective velocities $u(\mathbf{x})$ on the hypersurface (x) . The effective volume absorbs the collective velocity profile and the form of hypersurface and cancels out in all particle number ratios. Therefore, the particle number ratios do not depend on the freeze-out details as long as the local thermodynamic parameters are independent of x . The concept of the effective volume and factorization property similar to Eq. (7) has been considered first in Ref. [11], repeatedly used for the analysis of particle number ratios (see, e.g., Ref. [12]) and recently generalized for a study of the averaged phase space densities [13] and entropy [14]. One can apply this concept also in a limited rapidity window [11, 13, 14].

The concept of the effective volume can be applied to calculate the hadronic composition at both chemical and thermal freeze-outs [12]. At the former one, which happens soon after hadronization, the chemically equilibrated hadronic composition is assumed to be established and frozen in further evolution. The chemical potential μ_i for any particle species i at the chemical freeze-out is entirely determined by chemical potentials e_q per a unit charge, ie. per unit baryon number B , strangeness S , electric charge Q , charm C , etc. It can be expressed as a scalar product:

$$\mu_i = \mathbf{q}_i \tilde{\mathbf{e}}; \quad (8)$$

where $\mathbf{q}_i = (fB_i; S_i; Q_i; C_i; \dots)_T$ and $\tilde{\mathbf{e}} = (f e_B; e_S; e_Q; e_C; \dots)_T$. Assuming constant temperature and chemical potentials on the chemical freeze-out hypersurface, the total quantum numbers $\mathbf{q} = (fB; S; Q; C; \dots)_T$ of the selected thermal part of produced hadronic system (e.g., in a rapidity interval near $y = 0$) with corresponding V_e can be calculated as $\mathbf{q} = V_e \int_{(x)} d^3(x) \mathbf{q}_i$.

For example:

$$B = V_e \int_{(x)} d^3(x) \sum_{i=1}^{X^n} \mathbf{q}_i B_i; \quad (9)$$

$$S = V_e \int_{(x)} d^3(x) \sum_{i=1}^{X^n} \mathbf{q}_i S_i; \quad (10)$$

$$Q = V_e \sum_{i=1}^{X^n} e_i^{eq}(T; \mu_i) Q_i \quad (11)$$

The potentials e_q are not independent. Thus, taking into account baryon, strangeness and electrical charges only and fixing the total strangeness S and the total electric charge Q , e_s and e_q can be expressed through baryonic potential e_B using Eqs. (10) and (11). Therefore the mean numbers of each particle and resonance species at chemical freeze-out are determined solely by the temperature T and baryonic chemical potential e_B .

In practical calculations, we use the phenomenological observation [15] that particle yields in central Au+Au or Pb+Pb collisions in a wide center-of-mass energy range $\sqrt{s_{NN}} = 2.2 - 200$ GeV can be described within the thermal statistical approach using the following parametrizations of the temperature and baryonic chemical potential [15]:

$$T(e_B) = a + be_B^2 + ce_B^4 \quad (12)$$

$$e_B(\sqrt{s_{NN}}) = \frac{d}{1 + e^{-\sqrt{s_{NN}}}} \quad (13)$$

$a = 0.166 - 0.002$ GeV, $b = 0.139 - 0.016$ GeV¹, $c = 0.053 - 0.021$ GeV³ and $d = 1.308 - 0.028$ GeV, $e = 0.273 - 0.008$ GeV¹.

The particle densities at the chemical freeze-out stage are too high (see, e.g., [12]) to consider particles as free streaming and associate this stage with the thermal freeze-out one. The mean particle numbers N_i^{th} at thermal freeze-out can be determined using the following procedure [12]. First, the temperature and chemical potentials at chemical freeze-out have to be fitted from the ratios of the numbers of (quasi)stable particles. The fitting procedure should account for the decays of all resonances as well as unstable particles in given experimental conditions (feed-down). The common factor, V_e^{ch} , and, thus, the absolute particle and resonance numbers can be fixed, e.g., from pion multiplicities. Within the concept of chemically frozen evolution these numbers are assumed to be conserved except for corrections due to decay of some part of short-lived resonances that can be estimated from the assumed chemical to thermal freeze-out evolution time. Then one can calculate the mean numbers of different particles and resonances reaching a (common) thermal freeze-out hypersurface. At a given thermal freeze-out temperature T_{th} these mean numbers can be expressed through the thermal effective volume V_e^{th} and the chemical potentials for each

particle species i^{th} which can no more be expressed in the form $\epsilon_i = \epsilon_i \tilde{\epsilon}$ valid only for chemically equilibrated systems. For a given parametrization of the thermal freeze-out hypersurface, the thermally effective volume V_e^{th} (and thus all i^{th}) can be fixed with the help of pion interferometry data.

In practical calculations we determine all macroscopic characteristics of a particle system with the temperature T and chemical potentials μ_i via a set of equilibrium distribution functions in the fluid element rest frame:

$$f_i^{\text{eq}}(p^0; T; \mu_i) = \frac{1}{(2\pi)^3} \frac{g_i}{\exp(p^0 - \mu_i/T) \pm 1}; \quad (14)$$

Eq. (5) for the particle number density then reduces to

$$n_i^{\text{eq}}(T; \mu_i) = 4 \int_0^{\infty} dp p^2 f_i^{\text{eq}}(p^0; T; \mu_i); \quad (15)$$

Using the expansion

$$f_i^{\text{eq}}(p^0; T; \mu_i) = \frac{g_i}{(2\pi)^3} \sum_{k=1}^{\infty} (\pm)^{k+1} \exp\left(k \frac{\mu_i}{T}\right) \exp\left(-k \frac{p^0}{T}\right); \quad (16)$$

the density can be represented in a form of a fast converging series:

$$n_i^{\text{eq}}(T; \mu_i) = \frac{g_i}{2\pi^2} m_i^2 T \sum_{k=1}^{\infty} \frac{(\pm)^{k+1}}{k} \exp\left(\frac{k \mu_i}{T}\right) K_2\left(\frac{k m_i}{T}\right); \quad (17)$$

where K_2 is the modified Bessel function of the second order.

We assume that the calculated mean particle numbers $N_i = n_i^{\text{eq}} V_e$ correspond to a grand canonical ensemble. The probability that the ensemble consists of N_i particles is thus given by Poisson distribution:

$$P(N_i) = \exp(-N_i) \frac{(N_i)^{N_i}}{N_i!}; \quad (18)$$

III. HADRON MOMENTUM DISTRIBUTIONS

We suppose that a hydrodynamic expansion of the reball ends by a sudden system breakup at given temperature and chemical potentials. In this case the momentum distribution of the produced hadrons keeps the thermal character of the equilibrium distribution (3). Similar to Eqs. (1), (2), this distribution is then calculated according to the Cooper-Frye formula [16]:

$$p^0 \frac{d^3 N_i}{d^3 p} = \int_{(\mathbf{x})} d^3 \mathbf{x} p f_i^{\text{eq}}(p^0(\mathbf{x}); T; \mu_i); \quad (19)$$

The integral in Eq. (19) can be calculated with the help of the invariant weight

$$W_{,i}(x;p) = p^0 \frac{d^6 N_i}{d^3 d^3 p} = n(x) p^0 f_i^{\text{eq}}(p^0, \mathbf{p}; T; i); \quad (20)$$

It is convenient to transform the four-vectors into the fluid element rest frame, e.g.,

$$\begin{aligned} n^0 &= n u = (n^0 - \mathbf{v} \cdot \mathbf{n}); \\ \mathbf{n} &= \mathbf{n} + (1 + \gamma)^{-1} (n^0 + \mathbf{n} \cdot \mathbf{v}) \mathbf{v} \end{aligned} \quad (21)$$

and calculate the weight in this frame:

$$W_{,i}(x;p) = W_{,i}(x;p) = n(x) p^0 f_i^{\text{eq}}(p^0; T; i); \quad (22)$$

Particularly, in the case when the normal four-vector $n(x)$ coincides with the fluid element flow velocity $u(x)$, i.e. $n = u = f[1; 0; 0; 0]_g$, the weight $W_{,i}(x;p) = p^0 f_i^{\text{eq}}(p^0; T; i)$ is independent of x and isotropic in the three-momentum \mathbf{p} . A simple and 100% efficient simulation procedure can then be realized in this frame and the four-momenta of the generated particles transformed back to the lab rest frame using the velocity field $\mathbf{v}(x)$:

$$\begin{aligned} p^0 &= (p^0 + \mathbf{v} \cdot \mathbf{p}); \\ \mathbf{p} &= \mathbf{p} + (1 + \gamma)^{-1} (p^0 + \mathbf{p} \cdot \mathbf{v}) \mathbf{v}; \end{aligned} \quad (23)$$

There are two well-known examples of the models giving $n(x) = u(x)$: the Bjorken model with hypersurface $\Sigma_B = (t^2 - z^2)^{1/2} = \text{const}$ and absent transverse flow and the model with hypersurface $\Sigma_H = (t^2 - x^2 - y^2 + z^2)^{1/2} = \text{const}$ and spherically symmetric Hubble flow. In general case $n(x)$ may differ from $u(x)$ and one should account for the $x-p$ correlation and the corresponding anisotropy due to the factor $n \cdot p$ even in the fluid element rest frame [17].

IV. GENERALIZATION OF THE COOPER-FRYE PRESCRIPTION

It is well known that the Cooper-Frye freeze-out prescription in Eq. (19) is not valid for the part of the freeze-out hypersurface characterized by a space-like normal four-vector n . In this case $n^0 < |\mathbf{n}|$ and so $n \cdot p < 0$ for some particle momenta thus leading to negative contributions to particle numbers. Usually, the negative contributions are simply rejected [18, 19]. This procedure however violates the continuity condition of the flow $\int u \cdot d\Sigma$ through the freeze-out hypersurface. The correct generalization of Eq. (19) has the form [18]:

$$p^0 \frac{d^3 N_i}{d^3 p} = \int_{(\mathbf{x})} d^3 \mathbf{x} n(\mathbf{x}) \cdot (\mathbf{x}; p) f_i^{\text{eq}}(T(\mathbf{x}); i(\mathbf{x})); \quad (24)$$

where

$$\begin{aligned} \mathcal{E}(\mathbf{x};p) &= p \cdot (1 - \mathcal{E}(\mathbf{x};p)) + u(\mathbf{x}) p \cdot u(\mathbf{x}) \mathcal{E}(\mathbf{x};p) - 1; \\ \mathcal{E}(\mathbf{x};p) &= 1 - p \cdot n(\mathbf{x}) [p \cdot u(\mathbf{x}) n(\mathbf{x}) - u^2(\mathbf{x})] \end{aligned} \quad (25)$$

$$\mathcal{E}(\mathbf{x}) = 1 \text{ for } x \geq 0, \quad \mathcal{E}(\mathbf{x}) = 0 \text{ for } x < 0.$$

Passing to the fluid element rest frames at each point \mathbf{x} and using Lorentz transformation properties of the quantities in Eq. (24), one arrives at the same form of the four-vector of particle flow as in the case of the freeze-out hypersurface with the time-like normal $n(\mathbf{x})$:

$$j(\mathbf{x}) = \frac{Z}{p_0} \int d^3p \mathcal{E}(\mathbf{x};p) f_i^{\text{eq}}(T(\mathbf{x}); \mu_i(\mathbf{x})) = \frac{Z}{p_0} \int d^3p f_i^{\text{eq}}(T(\mathbf{x}); \mu_i(\mathbf{x})) u(\mathbf{x}) \quad (26)$$

Therefore the factorization of the freeze-out details in the effective volume in the case of constant temperature and chemical potentials, i.e. Eq. (7), is valid for any type of hypersurface [13].

It follows from Eqs. (24), (25) that the invariant weight in the fluid element rest frame has the form :

$$W_{\mu}(\mathbf{x};p) = p \cdot n \cdot \left[1 - \frac{p \cdot n}{p \cdot h} \right] + p \cdot h \cdot \left[\frac{p \cdot n}{p \cdot h} - 1 \right] f_i^{\text{eq}}(p \cdot u; T; \mu_i) \quad (27)$$

For the time-like normal $n(\mathbf{x})$, Eq. (27) reduces to Eq. (22).

It is worth noting that though the bulk of particles is likely associated with the volume decay, the particle emission from the surface of expanding system, or formally, from a non-space-like part of the freeze-out hypersurface enclosed in Minkowski space, is essential for a description of hadronic spectra and like pion correlations at relatively large p_T [20].

V. FREEZE-OUT SURFACE PARAMETERIZATIONS

At relativistic energies, due to dominant longitudinal motion, it is convenient to substitute the Cartesian coordinates t, z by the Bjorken ones

$$\tau = (\tau^2 - z^2)^{1/2}; \quad \eta = \frac{1}{2} \ln \frac{t+z}{t-z} \quad (28)$$

and introduce the the radial vector $\mathbf{x} = (r \cos \phi; r \sin \phi)$, i.e.:

$$x = \tau \cosh \eta; \quad z = \tau \sinh \eta; \quad r = \tau \cosh \phi; \quad y = \tau \sinh \phi; \quad \sinh \eta = \frac{z}{\tau} \quad (29)$$

Similarly, it is convenient to parameterize the fluid four-velocity $u(x) = (x) f_1; \mathbf{v}(x) g$ at a point x in terms of the longitudinal (z) and transverse (r) fluid rapidities

$$u(x) = \frac{1}{2} \ln \frac{1 + v_z(x)}{1 - v_z(x)}; \quad u(x) = \frac{1}{2} \ln \frac{1 + v_r(x) \cosh u(x)}{1 - v_r(x) \cosh u(x)}; \quad (30)$$

where $v_r = |\mathbf{v}_r|$ is the magnitude of the transverse component of the flow three-velocity $\mathbf{v} = f v_r \cos u; v_r \sin u; v_z g$, i.e.

$$\begin{aligned} u(x) &= f \cosh u \cosh u; \sinh u \cos u; \sinh u \sin u; \cosh u \sinh u g \\ &= f (1 + u_r^2)^{1/2} \cosh u; \mathbf{v}_r; (1 + u_r^2)^{1/2} \sinh u g; \end{aligned} \quad (31)$$

$\mathbf{v}_r = \mathbf{v}_r = r \cosh u \mathbf{v}_r, \quad r = \cosh u$. For the considered central collisions of symmetric nuclei, $u = 0$. Representing the freeze-out hypersurface by the equation $\tau = \tau(r)$; the hypersurface element in terms of the coordinates τ, r , becomes

$$d^3 = \frac{dx \, dx \, dx}{d \, dr \, d\tau}; \quad (32)$$

where ϵ_{0123} is the completely antisymmetric Levy-Civita tensor in four dimensions with $\epsilon_{0123} = \epsilon_{1230} = 1$. Particularly, for azimuthally symmetric hypersurface $\tau = \tau(r)$, Eq. (32) yields [12]:

$$d^3 = (\tau; r) d\tau dr d\phi \left[-\frac{1}{d} \sinh u + \cosh u; \frac{d}{dr} \cos u; \frac{d}{dr} \sin u; -\frac{1}{d} \cosh u \sinh u g \right]; \quad (33)$$

Generally, the freeze-out hypersurface is represented by a set of equations $\tau = \tau_j(r; \phi)$ and Eq. (32) should be substituted by the sum of the corresponding hypersurface elements.

To simplify the situation, besides the azimuthal symmetry, we further assume the longitudinal boost invariance [21]. The local quantities (such as particle density) are then functions of τ and r only. The hypersurface then takes the form $\tau = \tau(r)$, the flow rapidities $u = u(r)$ (i.e. $v_z = z = \tau$), $u = u(r)$ and Eq. (33) yields

$$\begin{aligned} d^3 &= (\tau) d\tau dr d\phi \left[f \cosh u; \frac{d}{dr} \cos u; \frac{d}{dr} \sin u; \sinh u g \right]; \\ d^3 &= \int_0^{2\pi} \left(\frac{d}{dr} \right)^2 \int_{-1}^1 (\tau) d\tau dr; \\ n(x) &= \int_0^{2\pi} \left(\frac{d}{dr} \right)^2 \int_{-1}^1 f \cosh u; \frac{d}{dr} \cos u; \frac{d}{dr} \sin u; \sinh u g; \end{aligned} \quad (34)$$

Note that the normal four-vector n becomes space-like ($n \cdot n = -1$) for $|\int_0^{2\pi} dr| > 1$.

For the simplest freeze-out hypersurface $\tau = \text{const}$ one has

$$\begin{aligned} d^3 &= d\tau dr d\phi; \\ n(x) &= f \cosh u; 0; 0; \sinh u g; \end{aligned} \quad (35)$$

In this case the normal $n(x)$ is time-like ($n \cdot n = 1$) but generally different from the flow four-velocity $u(x)$ except for the case of absent transverse flow (i.e. $u_{\perp} = 0$). Assuming $u_{\perp} = 0$ and the linear transverse flow rapidity profile:

$$u_{\perp} = \frac{r}{R} u_{\perp}^{\max}; \quad (36)$$

where R is the freeze-out transverse radius, the total effective volume for particle production at $\tau = \text{const}$ is

$$\begin{aligned} V_e &= \int_{(x)} d^3(x) u(x) = \int_0^R r dr \int_0^{z_{\max}} dz \int_{z_{\min}}^{z_{\max}} dz = \\ &= 2 \frac{R^2}{u_{\perp}^{\max}} \left(u_{\perp}^{\max} \sinh u_{\perp}^{\max} \cosh u_{\perp}^{\max} + 1 \right); \end{aligned} \quad (37)$$

where $z_{\min} = z_{\max} - u_{\perp}^{\max}$. For small values of the maximal transverse flow rapidity u_{\perp}^{\max} , Eq. (37) reduces to $V_e = R^2 \tau$ [12].

We shall refer the above choice of the freeze-out hyper-surface and the flow four-velocity profile as the Bjorken-like parametrization or Bjorken model scenario for particle freeze-out with transverse flows [21].

We also consider so called Craow model scenario [8] corresponding to the Hubble-like freeze-out hypersurface $H = (t^2 - x^2 - y^2 - z^2)^{1/2} = \text{const}$ and flow four-velocity

$$u(x) = x = H: \quad (38)$$

Introducing the longitudinal space-time rapidity η according to Eq. (28) and the transverse space-time rapidity $\xi = \sinh^{-1}(r/H)$, one has [22]

$$x = H \cosh \eta \cosh \xi; \quad \sinh \eta \cosh \xi; \quad \sinh \eta \sinh \xi; \quad \sinh \eta \cosh \xi; \quad (39)$$

$H = R \cosh \eta$. Representing the freeze-out hypersurface by the equation $H = H(\eta; \xi) = \text{const}$, one finds from Eq. (32):

$$\begin{aligned} d^3 &= H^3 \sinh \eta \cosh \eta d\eta d\xi d\xi = H d\eta d^2\xi; \\ n(x) &= u(x): \end{aligned} \quad (40)$$

The effective volume corresponding to $r = H \sinh \xi < R$ and $z_{\min} = z_{\max}$ is

$$V_e = \int_{(x)} d^3(x) u(x) = \int_H^R r dr \int_0^{z_{\max}} dz \int_{z_{\min}}^{z_{\max}} dz = H R^2 \tau: \quad (41)$$

VI. HADRON GENERATION PROCEDURE

Our MC procedure to generate the freeze-out hadron multiplicities, four-momenta and four-coordinates is the following:

1. First, the parameters of the chosen freeze-out model are initialized. Particularly, for the models with constant freeze-out temperature T and chemical potentials μ_i , the phenomenological formulae (12), (13) are implemented as an option allowing to calculate T and μ_i at the chemical freeze-out in central Au + Au or Pb + Pb collisions specifying only the center-of-mass energy $\sqrt{s_{NN}}$. In the scenario with the thermal freeze-out occurring at a temperature $T^{\text{th}} < T^{\text{ch}}$, the chemical potentials μ_i^{th} are no more given by Eq. (8). At given thermal freeze-out temperature T^{th} and effective volume V_e^{th} , they are set according to the procedure described in section II. So far, only the stable particles and resonances consisting of u, d, s quarks are incorporated in the model. They are taken from the ROOT particle data table [6, 23].
2. Next, the effective volume corresponding to a given freeze-out model is determined, e.g., according to Eq. (37) or (41) and particle number densities are calculated with the help of Eq. (17). The mean multiplicity of each particle species is then calculated according to Eq. (7). A more general option to calculate the mean multiplicities, e.g., in the case of the freeze-out hypersurface obtained from relativistic hydrodynamics, is the direct integration of Eq. (24). The multiplicity corresponding to the mean one is simulated according to Poisson distribution in Eq. (18).
3. The particle freeze-out four-coordinates x are then simulated according to weight $d^3x = n^0(r) r dr d\Omega$, assuming n^0 to be only a function of r (i.e. independent of θ, ϕ), by sampling uniformly distributed r in the interval $[r_{\text{min}}; r_{\text{max}}]$, θ in the interval $[0; 2\pi]$ and generating ϕ in the interval $[0; R]$ using a 100% efficient procedure similar to ROOT routine `GetRandom()`. In the Bjorken-like model $n^0 = \cosh u = \cosh \eta$, while in the Hubble-like model $n^0 = 1$. Note that if n^0 were depending on two or three variables, a generalization of the routine `GetRandom()` to more dimensions is possible. A less efficient possibility, realized in the case when the particle freeze-out four-coordinates x and the corresponding hypersurface normal four-vectors $n(x)$ and

collective four-velocities $u(x)$ are calculated from relativistic hydrodynamics, is the inclusion of the factor n^0 in the residual weight in the step 6.

4. The corresponding collective flow four-velocities $u(x)$ are calculated using, e.g., Eqs. (31), (36) or Eq. (38).
5. The particle three-momenta $p = p_T (\cos \phi; \sin \phi; \cos \eta)$ are then generated in the fluid element rest frames according to the probability $f_i^{\text{eq}}(p^0; T; \mu_i) p^2 dp d\cos \theta_p d\phi_p$ by sampling uniformly distributed $\cos \theta_p$ in the interval $[-1; 1]$, ϕ_p in the interval $[0; 2\pi]$ and generating p using a 100% efficient procedure similar to ROOT routine `GetRandom()`.
6. Next, the standard von Neumann rejection/acceptance procedure is used to account for the difference between the true weight $W_i d^3 p = p^0$ (see Eqs. (20), (22), (27)) and the weight $n^0 f_i^{\text{eq}}(p^0; T; \mu_i) d^2 p$ corresponding to the simulation steps 3-5. Thus the residual weight

$$W_i^{\text{res}} = \frac{W_i d^3 p}{n^0 p^0 f_i^{\text{eq}} d^2 p} \quad (42)$$

is calculated and the simulated particle four-coordinate and four-momentum are accepted provided this weight is larger than a test variable randomly simulated in the interval $[0; \max(W_i^{\text{res}})]$. Otherwise, the simulation returns to step 3. Note that for the freeze-out parametrizations considered in this paper,

$$W_i^{\text{res}} = 1 - \frac{n p}{n^0 p^0} \quad (43)$$

and the maximal weight $\max(W_i^{\text{res}})$ can be calculated analytically. Particularly, in the Bjorken-like model and $\mu^{\text{ax}} = 1$, W_i^{res} is distributed in the interval $[1 - \tanh \frac{\mu^{\text{ax}}}{u}; 1 + \tanh \frac{\mu^{\text{ax}}}{u}]$. The step 6 can be omitted for the Hubble-like model or for the Bjorken model without transverse flow ($u = 0$) when $W_i^{\text{res}} = 1$. Also note that in the case when the particle freeze-out four-coordinates are calculated from relativistic hydrodynamics, the residual weight should include the factor n^0 and take into account the contribution of non-space-like sectors of the freeze-out hypersurface:

$$W_i^{\text{res}} = n^0 \left[1 - \frac{n p}{n^0 p^0} \right] + \frac{p n}{p^0 n^0} \quad (44)$$

7. Next, the hadron four-momentum p is boosted to the lab rest frame according to Eqs. (23).

8. The two-body, three-body and many-body decays are simulated with the branching ratios calculated via ROOT utilities [6]. A more correct kinetic evolution, taking into account not only resonance decays but also hadron elastic scattering, may be included with the help of the Boltzmann equation solver C++ code which was developed earlier [24].

It should be stressed that a high generation speed is achieved due to 100% generation efficiency of the freeze-out four-coordinates and four-momenta in steps 3-5 as well as due to a weak non-uniformity of the residual weight W_i^{res} in the cases of practical interest. For example, in the Bjorken-like model, the increase of the maximal transverse flow rapidity from zero ($W_i^{res} = \text{const}$) to $u^{max} = 0.65$ leads only to a few percent decrease of the generation speed. Compared, e.g., to THERMINATOR [9], our generator appears more than one order of magnitude faster.

VII. VALIDATION OF THE MC PROCEDURE

In the Boltzmann approximation for the equilibrium distribution function (14), i.e. retaining only the first term in the expansion (16), the transverse momentum (p_t) spectrum in the Bjorken-like model takes the form [2, 25]:

$$\frac{dN_i}{p_t dp_t} = \frac{1}{-g_i} m_t e^{i=T} \int_0^{Z_R} r dr K_1 \left(\frac{m_t \cosh u}{T} \right) I_0 \left(\frac{p_t \sinh u}{T} \right); \quad (45)$$

where $I_0(z)$ and $K_1(z)$ are the modified Bessel functions and $m_t = (m_i^2 + p_t^2)^{1/2}$ is the particle transverse mass.

To test our MC procedure, we compare in Fig. 1 the transverse momentum spectrum calculated according to Eq. (45) with the corresponding MC result for $T = 0.165$ GeV, $R = 8$ fm, $m_i = 0.14$ GeV, $\mu = 10$, $\mu = 0.0$ GeV, $\beta = 12$ fm/c, $u^{max} = 0.65$ and 2.0. One may see that the analytical and the MC calculations practically coincide.

To demonstrate the increasing influence of the residual weight with the increasing u^{max} , we also present in Fig. 1 the MC results obtained without this weight.

V III. INPUT PARAMETERS AND EXAMPLE CALCULATIONS

We present here the results of example MC calculations performed on the assumption of a common chemical and thermal freeze-out and compare them with the experimental data on central Au + Au collisions at RHIC.

A. Model input parameters

First, we summarize the input parameters which control the execution of our MC hadron generator in the case of Bjorken-like and Hubble-like parametrizations with a common thermal and chemical freeze-out:

1. Number of events to generate.
2. Thermodynamic parameters at chemical freeze-out: temperature (T) and chemical potentials per a unit charge ($e_B; e_S; e_Q$). As an option, there is an additional parameter $s = 1$ taking into account the strangeness suppression according to partially equilibrated distribution [26, 27]:

$$f_i(p^0; T; \mu_i; s) = \frac{g_i}{s^{n_i^s} \exp((p^0 - \mu_i)/T)^{1/s}}; \quad (46)$$

where n_i^s is the number of strange quarks and anti-quarks in a hadron i . Optionally, the parameter s can be fixed using its phenomenological dependence on the temperature and baryon chemical potential [28].

3. Volume parameters: the freeze-out proper time (τ) and initial transverse radius (R).
4. Maximal transverse flow rapidity (η_u^{max}) for Bjorken-like parametrization [2, 3].
5. Maximal space-time longitudinal rapidity (η_{max}) which determines the rapidity interval $[\eta_{-max}; \eta_{max}]$ in the collision center-of-mass system. To account for the violation of the boost invariance, we have included in the code an option corresponding to the substitution of the uniform distribution of the space-time longitudinal rapidity in the interval $[\eta_{-max}; \eta_{max}]$ by a Gaussian distribution $\exp(-\eta^2/2\sigma^2)$ with a width parameter σ (see, e.g., [29]).

The parameters used to model central Au+Au collisions at $\sqrt{s_{NN}} = 200$ GeV are given in Table I.

TABLE I: The model parameters for central Au + Au collisions at $\sqrt{s_{NN}} = 200$ GeV.

parameter	Bjorken-like	Hubble-like
$T, \text{ GeV}$	0.165	0.165
$e_B, \text{ GeV}$	0.028	0.028
$e_S, \text{ GeV}$	0.007	0.007
$e_Q, \text{ GeV}$	-0.001	-0.001
s	1 (0.8)	1 (0.8)
$r, \text{ fm}/c$	6.1	9.65
$R, \text{ fm}$	10.0	8.2
m_{ax}	2 (3,5)	2 (3,5)
m_{ax}^u	0.65	-

B. Space-time distributions of the hadron emission points

In figures 2 and 3, we show the distributions of the π^+ emission transverse x-coordinate and time generated in the Bjorken-like and Hubble-like models with the parameters given in Table I, $m_{ax} = 2$. Also shown are the contributions from the primary π^+ 's emitted directly from the freeze-out hypersurface and the contributions from π^+ 's from the decays of the most abundant resonances $\rho, \omega, K^*(892)$ and Δ . For primary pions, $x < R$ and $0 < t < \cosh m_{ax}$. The tails at $|x| > R$ and $t > \cosh m_{ax}$ reflect the exponential law of the resonance decays. The longest tails in figures 2 and 3 are due to pions from Δ decays.

C. Ratios of hadron abundances

It is well known that the particle abundances in heavy-ion collisions in a large energy range can be reasonably well described within statistical models (see, e.g., [26, 30, 31]) based on the assumption that the produced hadronic matter reaches thermal and chemical equilibrium. This is demonstrated in tables II and III for the particle number ratios near mid-rapidity in central Au + Au collisions at $\sqrt{s_{NN}} = 130$ and 200 GeV calculated in our MC model and the statistical model of Ref. [32] and compared with the RHIC experimental data. Being independent of volume and flow parameters, the particle number ratio allow one

TABLE II: Particle number ratios near mid-rapidity in central Au + Au collisions at $\sqrt{s_{NN}} = 130$ GeV calculated with the thermodynamic parameters: $T = 0.168$ GeV, $e_B = 0.041$ GeV, $e_S = 0.010$ GeV and $e_Q = 0.001$ GeV.

particle number ratios	our M C	statistical model [32]	experiment
π^+/π^-	0.98	1.02	1.00 ± 0.02 [33], 0.99 ± 0.02 [34]
p/\bar{p}	0.06	0.09	0.08 ± 0.01 [35]
K^0/\bar{K}^0	0.90	0.92	0.91 ± 0.09 [33], 0.93 ± 0.07 [36]
K^+/\bar{K}^+	0.22	0.16	0.15 ± 0.02 [37]
p/\bar{p}	0.61	0.65	0.60 ± 0.07 [33], 0.64 ± 0.08 [36]
$\Lambda/\bar{\Lambda}$	0.69	0.69	0.71 ± 0.04 [38]
$\Sigma/\bar{\Sigma}$	0.79	0.77	0.83 ± 0.06 [38]
$\Xi/\bar{\Xi}$	0.17	0.15	0.13 ± 0.03 [39]
$\Xi/\bar{\Xi}$	0.48	0.47	0.49 ± 0.03 [40], [41]
$\Omega/\bar{\Omega}$	0.0086	0.0072	0.0088 ± 0.0020 [42]

TABLE III: Particle number ratios near mid-rapidity in central Au + Au collisions at $\sqrt{s_{NN}} = 200$ GeV calculated with the thermodynamic parameters: $T = 0.165$ GeV, $e_B = 0.028$ GeV, $e_S = 0.07$ GeV, and $e_Q = 0.001$ GeV.

particle number ratios	our M C	experiment [44]
π^+/π^-	0.98	0.984 ± 0.004
K^0/\bar{K}^0	0.94	0.933 ± 0.008
K^+/\bar{K}^+	0.21	0.162 ± 0.001
p/\bar{p}	0.71	0.731 ± 0.011

to fix the thermodynamic parameters. We have not tuned the latter here and simply used the same thermodynamic parameters as in Ref. [32] despite there are noticeable differences in some particle number ratios calculated in the two models. These differences may be related to the different numbers of resonance states taken into account and uncertainties in the decay modes of high excited resonances.

D . Pseudo-rapidity distributions

In Fig. 4, we compare the PHOBOS data [43] on pseudo-rapidity spectrum of charged hadrons in central Au+Au collisions at $\sqrt{s_{NN}} = 200$ GeV with our MC results obtained within the Bjorken-like and Hubble-like models for different values of m_{ax} . One may see that the data are compatible with the longitudinal boost invariance only in the mid-rapidity region in which the model is practically insensitive to m_{ax} . In the single freeze-out scenario, the data on particle numbers at mid-rapidity thus allows one to fix the effective volume V_e / R^2 .

E . Transverse momentum spectra

In Fig. 5, we compare the mid-rapidity PHENIX data [44] on π^+ , K^+ and proton p_t spectra in Au+Au collisions at $\sqrt{s_{NN}} = 200$ GeV with our MC results obtained within the Bjorken-like and Hubble-like models. A good agreement between the models and the data may be seen for pions while for kaons and protons the models overestimate the spectra at $p_t < 1$ GeV/c. For kaons, this discrepancy can be diminished with the help of the strangeness suppression parameter s of 0.8 (see the right panel in Fig. 5). The overestimated slope of the kaon and proton p_t spectra can also be related with the oversimplified assumption of a common thermal and chemical freeze-out or insufficient number of the accounted heavy resonance states.

The contribution of different resonances to the pion p_t spectrum calculated in the Bjorken-like model is shown in Fig. 6.

Note that in Hubble-like model, the transverse flow is determined by the volume parameters R ; and so, at fixed thermodynamic parameters and the effective volume V_e / R^2 , the transverse momentum spectra allow one to fix both R and β . In the Bjorken-like model, there is more freedom since the transverse flow is also regulated by the parameter m_{u}^{ax} . The choice of these parameters in Table I has been done to minimize the discrepancy of the simulated and measured correlation radii of identical pions (see below).

F. Correlation functions

It is well known that, due to the effects of quantum statistics (QS) and final state interaction (FSI), the momentum correlations of two or more particles at small relative momenta in their center-of-mass system are sensitive to the space-time characteristics of the production process on a level of $m = 10^{-15}$ m so serving as a correlation femtoscopy tool (see, for example, [45]–[49]).

The momentum correlations are usually studied with the help of correlation functions of two or more particles. Particularly, the two-particle correlation function $CF(p_1; p_2)$ is defined as a ratio of the measured two-particle distribution to the reference one which is usually constructed by mixing the particles from different events of a given class, normalizing the correlation function to unity at sufficiently large relative momenta.

Since our MC generator provides the information on particle four-momenta p_i and four-coordinates x_i of the emission points, it can be used to calculate the correlation function with the help of the weight procedure, assigning a weight to a given particle combination accounting for the effects of QS and FSI. Here we will consider the correlation function of two identical pions neglecting their FSI, so the weight

$$w = 1 + \cos(q \cdot x); \quad (47)$$

where $q = p_1 - p_2$ and $x = x_1 - x_2$. The CF is defined as a ratio of the weighted histogram of the pair kinematic variables to the unweighted one.

Generally, the pair is characterized by six kinematic variables. In case of the azimuthal symmetry, there are five variables that are usually chosen as the three "out-side-long" components of the relative three-momentum vector [46, 47] $q = (q_{out}; q_{side}; q_{long})$, half the pair transverse momentum k_t and the pair rapidity or pseudo-rapidity. The out and side denote the transverse, with respect to the reaction axis, components of the vector q ; the out direction is parallel to the transverse component of the pair three-momentum.

The corresponding correlation widths are usually parameterized in terms of the Gaussian correlation radii R_i ,

$$CF(p_1; p_2) = 1 + \exp(-R_{out}^2 q_{out}^2 - R_{side}^2 q_{side}^2 - R_{long}^2 q_{long}^2 - 2R_{out;long}^2 q_{out} q_{long}) \quad (48)$$

and their dependence on pair rapidity and transverse momentum is studied. The form of Eq. (48) assumes azimuthal symmetry of the production process [46]. Generally, e.g., in

case of the correlation analysis with respect to the reaction plane, all three cross terms $q_i q_j$ contribute [29]. We choose as the reference frame the longitudinal co-moving system (LCMS) [48]. In LCMS each pair is emitted transverse to the reaction axis so that the pair rapidity vanishes. The parameter α measures the correlation strength. For fully chaotic Gaussian source $\alpha = 1$. Experimentally observed values of $\alpha < 1$ are mainly due to contribution of very long-lived sources (τ , 0 , K_s^0 , \dots), the non-Gaussian shape of the correlation functions and particle misidentification.

The correlation functions of two identical charged pions have been calculated within the Bjorken-like and Hubble-like models with the parameters given in Table I, $m_{ax} = 2$, reasonably well describing single particle spectra in the mid-rapidity region. The three-dimensional correlation functions were fitted according to Eq. (48) in two k_t intervals $0.1 < k_t < 0.3$ GeV/c and $0.3 < k_t < 0.6$ GeV/c. In Fig. 7, the fitted correlation radii and strength parameter are compared with those measured by STAR collaboration [49]. One may see that the Bjorken-like model, adjusted to describe single particle spectra, describes also the decrease of the correlation radii with increasing k_t but overestimates their values. The situation is even worse with the Hubble-like model which is more constraint than the Bjorken-like one and yields the longitudinal radius by a factor two larger.

As for the overestimation of the correlation strength parameter α , it is likely related to the neglected contribution of misidentified particles and pions from weak decays. Indeed, the new preliminary analysis of the STAR data with the improved particle identification [50] yields the α parameter closer to the model results.

We would like to emphasize that the high freeze-out temperature of 165 MeV and a fixed effective volume V_e / R^2 make it quite difficult to describe the correlation radii within the single freeze-out model. Thus a tuning of the longitudinal radius $R_{long} \propto (T - m_t)^{1=2}$ requires a small proper time τ , leading to too large values of R and R_{side} / R . The concept of a later thermal freeze-out occurring at a smaller temperature $T^{th} < T^{ch}$ and with no multiplicity constraint on the thermal effective volume (see section II) can help to resolve this problem (see, e.g., [7]).

To get a valuable information from the correlation data, one should consider more realistic models as compared with the simple Bjorken-like and Hubble-like ones (particularly, consider a more complex form of the freeze-out hypersurface taking into account particle emission from the surface of expanding system [20]) and study the problem of particle rescattering

and resonance excitation after the chemical and/or thermal freeze-out (only minor effect of elastic rescatterings on particle spectra and correlations is expected [24]). For the latter, our earlier developed C++ kinetic code [24] can be coupled to the MC freeze-out generator.

IX . CONCLUSIONS AND PERSPECTIVES

We have developed a MC simulation procedure and the corresponding C++ code allowing for a fast but realistic description of multiple hadron production in central relativistic heavy ion collisions. A high generation speed and an easy control through input parameters make our MC generator code particularly useful for detector studies. As options, we have implemented two freeze-out scenarios with coinciding and with different chemical and thermal freeze-outs. Also implemented are various options of the freeze-out hypersurface parameterizations including those with non-space-like hypersurface sectors related to the emission from the surface of expanding system. The generator code is quite flexible and allows the user to add other scenarios and freeze-out surface parameterizations as well as additional hadron species in a simple manner.

We have compared the RHIC experimental data with our MC generation results obtained within the single freeze-out scenario and Bjorken-like and Hubble-like freeze-out surface parameterizations. While simplified, such a scenario nevertheless allows for a reasonable description of particle spectra. It however fails to describe the correlation functions of identical pions, overestimating the correlation radii.

The RHIC data thus points to the need for a more complicated scenario likely including different chemical and thermal freeze-outs, a more complex form of the freeze-out hypersurface (the use of numerical solution of the relativistic hydrodynamics is foreseen) and the account for kinetic evolution following the chemical and/or thermal freeze-out (for this, the MC generator can be coupled to our C++ kinetic code [24]).

We plan to implement in the MC generator the in-pair parameter dependence of the freeze-out hypersurface and account for the anisotropic flow similar to Ref. [4, 5]. In view of the importance of high- p_t physics related to the partonic states created in ultra-relativistic heavy ion collisions, we also foresee the inclusion of mini-jet production [5].

Acknowledgments

We would like to thank B.V. Batyunia and L.I. Sarycheva for useful discussions. The research has been carried out within the scope of the ERG (GDRE): Heavy ions at ultra-relativistic energies – a European Research Group comprising IN2P3/CNRS, Ecole des Mines de Nantes, Université de Nantes, Warsaw University of Technology, JINR Dubna, ITP Moscow and Bogolyubov Institute for Theoretical Physics NAS of Ukraine. This work has been supported, in part, by Grant of Russian Agency for Science and Innovations under contract 02.434.11.7074 (2005-R I-12.0/004/022), by the special program of the Ministry of Science and Education of the Russian Federation, grant RNP 2.1.1.5409, by the Grant Agency of the Czech Republic under contract 202/04/0793 and by Award No. UKP1-2613-KV-04 of the U.S. Civilian Research and Development Foundation (CRDF) and Fundamental Research State Fund of Ukraine, Agreement No. F7/209-2004.

-
- [1] Proc. of the Conference "Quark Matter 2005", Nucl. Phys. A 774 (2006).
 - [2] I.P. Lokhtin and A.M. Snigirev, Phys. Lett. B 378, 247 (1996).
 - [3] N.A. Kruglov, I.P. Lokhtin, L.I. Sarycheva and A.M. Snigirev, Z. Phys. C 76, 99 (1997).
 - [4] I.P. Lokhtin and A.M. Snigirev, Preprint SINP MSU 2004-14/753, hep-ph/0312204.
 - [5] I.P. Lokhtin and A.M. Snigirev, Eur. Phys. J. C 45, 211 (2006).
 - [6] R. Brun and F. Rademakers, Nucl. Instrum. Meth. A 389, 81 (1997), (<http://root.cern.ch>).
 - [7] F. Retiere and M. Lisa, Phys. Rev. C 70, 044907 (2004).
 - [8] W. Florkowski and W. Broniowski, Acta. Phys. Pol. 35, 2855 (2004).
 - [9] THERMINATOR: Thermal heavy-ion generator, A. Kisiel, T. Taluc, W. Broniowski, W. Florkowski, nucl-th/0504047.
 - [10] S.R. de Groot, W.A. van Leeuwen, Ch.G. van Weert, Relativistic kinetic theory. Principles and Applications, North-Holland Publishing Company, Amsterdam-New York-Oxford, 1980.
 - [11] Yu.M. Sinyukov, S.V. Akkelin and A.Yu. Tolstykh, Nukleonika 43, 369 (1998).
 - [12] S.V. Akkelin, P. Braun-Munzinger and Yu.M. Sinyukov, Nucl. Phys. A 710, 439 (2002).
 - [13] S.V. Akkelin and Yu.M. Sinyukov, Phys. Rev. C 70, 064901 (2004).
 - [14] S.V. Akkelin and Yu.M. Sinyukov, Phys. Rev. C 73, 034908 (2006).

- [15] J. Cleymans, H. Oeschler, K. Redlich and S. Wheaton, J. Cleymans, H. Oeschler, K. Redlich, S. W heaton, Phys. Rev. C 73, 034905 (2006).
- [16] F. Cooper and G. Frye, Phys. Rev. D 10, 186 (1974).
- [17] M. I. Gorenstein and Yu M. Sinyukov, Phys. Lett. B 142, (1985) 425.
- [18] Yu M. Sinyukov, Z. Phys. C 43, 401 (1989).
- [19] K. A. Bugaev, Nucl. Phys. A 606, 559 (1996); C. S. Anderlik et al., Phys. Rev. C 59, 3309 (1999).
- [20] M. S. Borysova, Yu M. Sinyukov, S. V. Akkelin, B. Erasmus and Iu A. Karpenko, Phys. Rev. C 73, 024903 (2006).
- [21] J. D. Bjorken, Phys. Rev. D 27, 140 (1983).
- [22] T. C. Sogo and B. Lorstad, Phys. Rev. C 34, 1340 (1996).
- [23] Particle Data Group, K. Hagiwara et al., Phys. Rev. D 66, 010001 (2002).
- [24] N. S. Amelin, R. Lednicky, L. V. Malinina, T. A. Pocheptsov and Y. M. Sinyukov, Phys. Rev. C 73, 044909 (2006).
- [25] E. Schnedermann, J. Sollfrank and U. Heinz, Phys. Rev. C 48, 2462 (1993).
- [26] G. Yen, M. I. Gorenstein, W. Greiner and S. N. Yang, Phys. Rev. C 56, 2210 (1997).
- [27] J. Rafelski, Phys. Lett. B 262, 333 (1981).
- [28] F. Becattini, J. Manninen, M. Gazdzicki, Phys. Rev. C 73, 044905 (2006).
- [29] U. A. Wiedemann and U. Heinz, Phys. Rept. 319, 145 (1999).
- [30] THERMUS { A Thermal Model Package for ROOT, S. W heaton and J. Cleymans, hep-ph/0407174.
- [31] P. Braun-Munzinger et al., Phys. Lett. B 344, 43 (1995), *ibid.* B 365, 1 (1996), *ibid.* B 465, 15 (1999).
- [32] W. Florkowski and W. Broniowski, AIP Conf. Proc. 660, 177 (2003); nucl-th/0212052 v1.
- [33] B. B. Back et al., PHOBOS Collaboration, Phys. Rev. Lett. 87, 102301 (2001).
- [34] I. G. Bearden et al., BRAHMS Collaboration, Nucl. Phys. A 698, 667c (2002).
- [35] J. Harris et al., STAR Collaboration, Nucl. Phys. A 698, 64c (2002).
- [36] H. Ohnishi et al., PHENIX Collaboration, Nucl. Phys. A 698, 659c (2002).
- [37] H. Caines et al., STAR Collaboration, Nucl. Phys. A 698, 112c (2002).
- [38] J. Adams et al., STAR Collaboration, Phys. Lett. B 567, 167 (2003).
- [39] C. Adler et al., STAR Collaboration, Phys. Rev. C 65, 041901 (2002).

- [40] C. Adler et al., STAR Collaboration, Phys. Rev. Lett. 89, 092301 (2002).
- [41] C. Adler et al., STAR Collaboration, Phys. Rev. Lett. 87, 262302 (2001).
- [42] J. Castillo et al., STAR Collaboration, nucl-ex/0210032.
- [43] B. B. Back et al., PHOBOS Collaboration, Nucl Phys. A 757, 28 (2005).
- [44] S. S. Adler et al., PHENIX Collaboration, Phys. Rev. C 69, 034909 (2004).
- [45] R. Lednicky, Proc. of the Conference "Quark Matter 2005", Nucl. Phys. A 774, 189 (2006).
- [46] M. I. Podgoretskii, Sov. J. Nucl. Phys. 37, 272 (1983).
- [47] S. Pratt, Phys. Rev. Lett. 53, 1219 (1984).
- [48] T. C. Sogor and S. Pratt, Proc. of the Workshop on Heavy Ion Physics, KFK I-1991-28/A, 75.
- [49] J. Adams et al., STAR Collaboration, Phys. Rev. C 71, 044906 (2005).
- [50] M. Bystersky, STAR Collaboration, AIP Conf. Proc. 828, 533 (2006); nucl-ex/0511053.

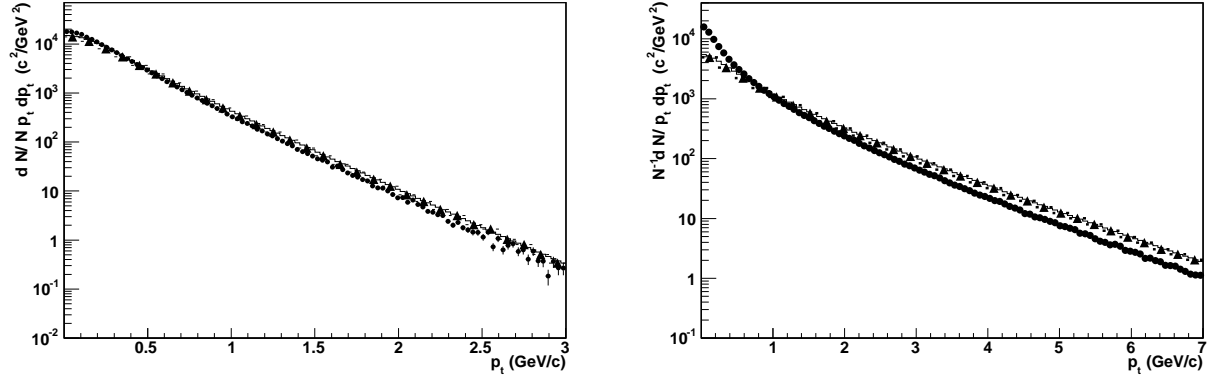


FIG .1: The validation of the MC procedure for $m_{ax}^m = 0.65$ (left panel) and 2.0 (right panel): the transverse momentum spectra (solid lines) calculated according to Eq. (45) and the corresponding MC results (black triangles). Also shown are the MC results obtained with a constant residual weight (black points).

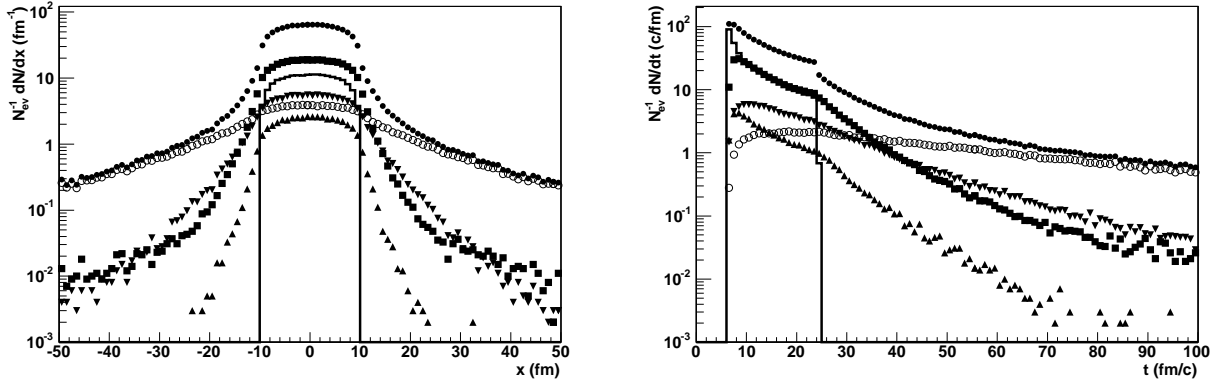


FIG .2: The $+$ emission transverse x -coordinate (left) and time (right) generated in the Bjorken-like model with the parameters given in Table I, $m_{ax}^m = 2$: all $+$'s (solid circles), direct $+$'s (solid line), decay $+$'s from (squares), ! (open circles), $K(892)$ (up-triangles) and (down-triangles).

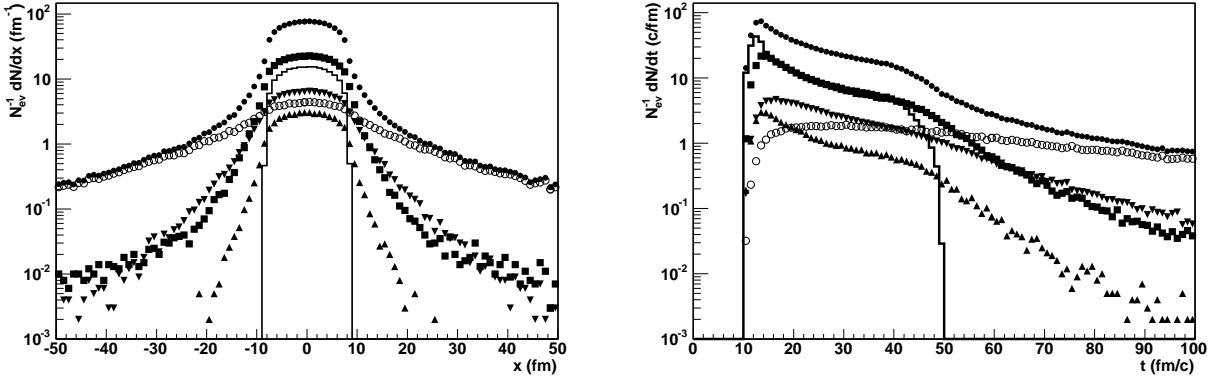


FIG . 3: The same as in Fig. 2 for the Hubble-like parameterization .

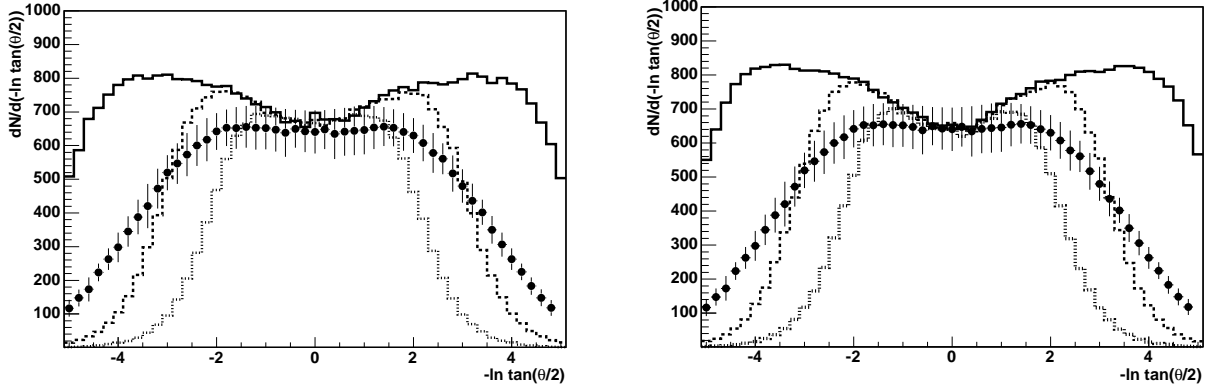


FIG . 4: The pseudo-rapidity ($-\ln \tan(\theta/2)$, θ is the particle production angle) distributions of charged particles in central Au + Au collisions at $\sqrt{s_{NN}} = 200$ GeV from the PHOBOS experiment [43] (solid circles) and the MC calculations within the Bjorken-like (left panel) and Hubble-like (right panel) models. The model results corresponding to the space-time rapidity range parameter $m_{ax} = 5; 3$ and 2 are shown by solid, dashed and dotted lines respectively.

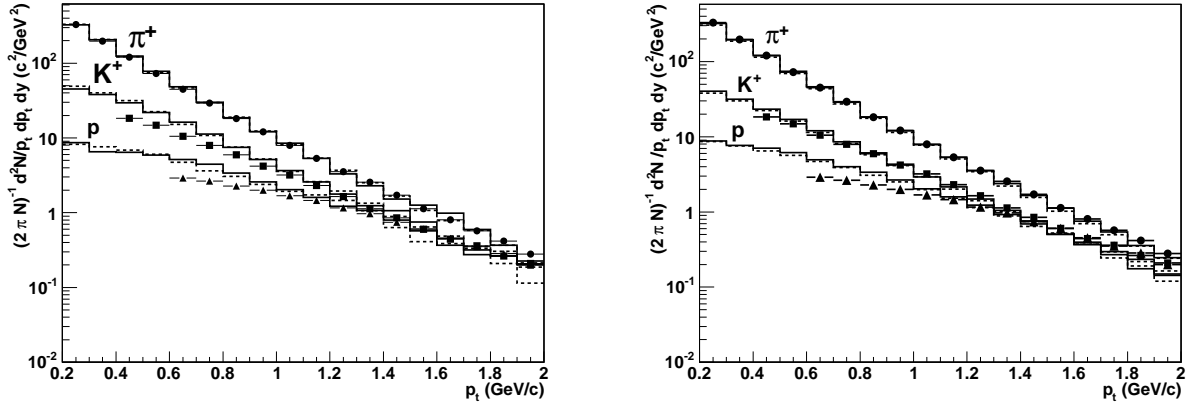


FIG. 5: The π^+ , K^+ and proton transverse momentum spectra at mid-rapidity $y = 0$ in central Au + Au collisions at $\sqrt{s_{NN}} = 200$ GeV from PHENIX experiment [44] (solid symbols) and the MC calculations within the Bjorken-like (dashed lines) and Hubble-like (solid lines) models. The right panel shows the model results obtained with the strangeness suppression parameter $s = 0.8$.

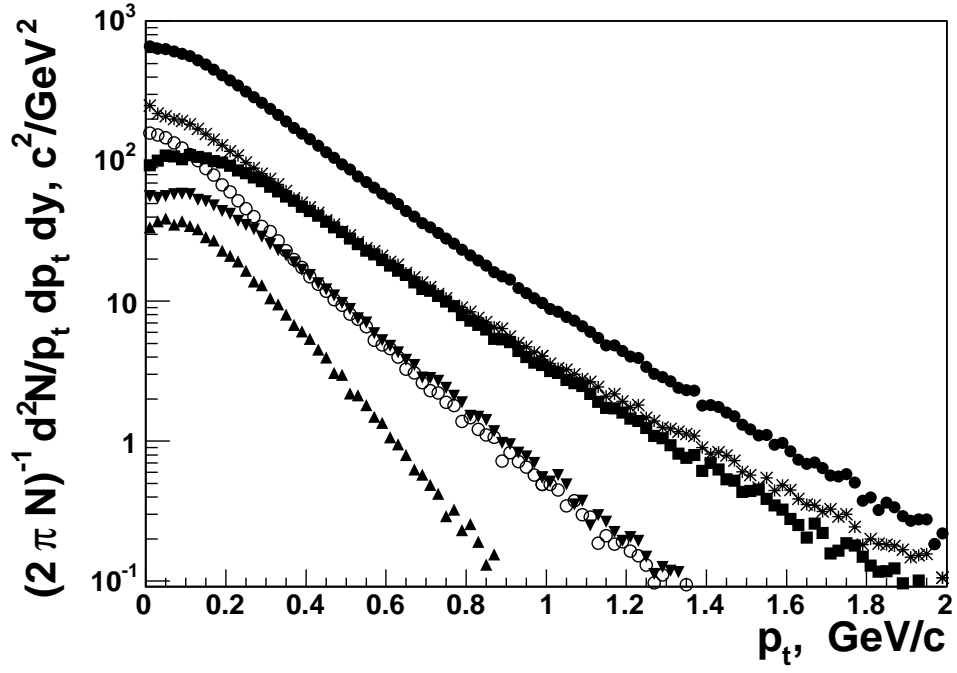


FIG. 6: The contributions to the p transverse momentum spectrum at mid-rapidity in central Au + Au collisions at $\sqrt{s_{NN}} = 200$ GeV calculated within the Bjorken-like model: all p 's (solid circles), direct p 's (stars), decay p 's from Λ (squares), Λ (open circles), K (892) (up-triangles) and Λ (down-triangles).

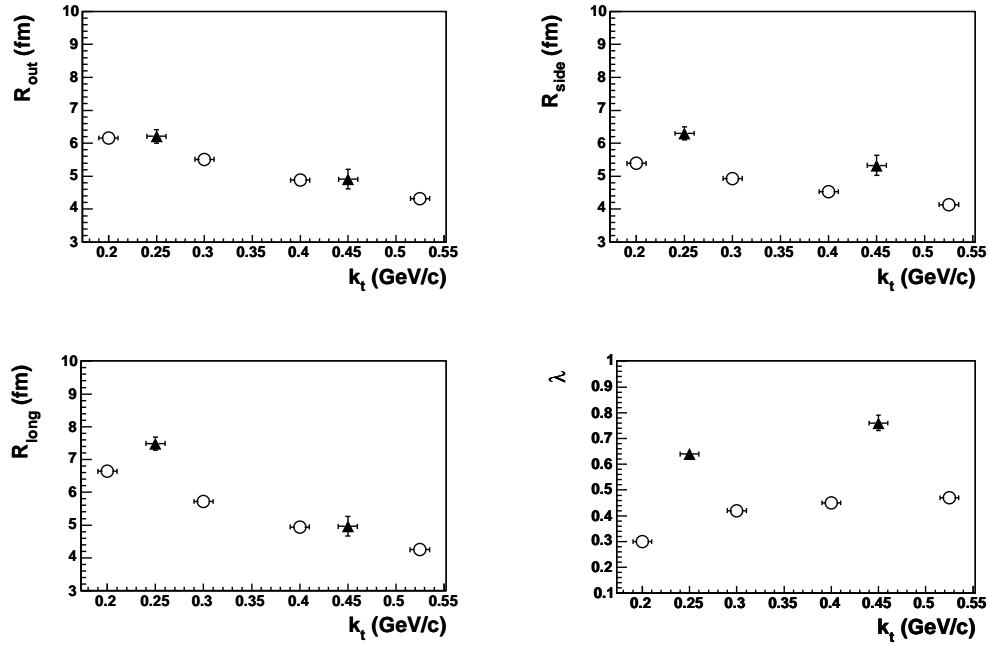


FIG. 7: The correlation radii and the suppression parameter at mid-rapidity in central Au + Au collisions at $\sqrt{s_{NN}} = 200$ GeV from the STAR experiment [49] (open circles) and the MC calculations within the Bjorken-like model (up-triangles) in different intervals of the pair transverse momentum k_t .